buildings

MDPI

Article

Integrated Evaluation of Bio-Based Phase Change Materials to Reduce Operational and Embodied Carbon in Service Buildings Across Multiple Climate Zones

Abdessamad Idouanaou *, Mustapha Malha, Saïd Kardellass, Abdellah Bah, Omar Ansari, Rabab El Attar and Oumayma Cherqi

Thermal and Energy Research Team, National Higher School of Arts and Crafts, Mohammed V University, Rabat B.P. 6207, Morocco; m.malha@um5r.ac.ma (M.M.); s.kardellass@um5r.ac.ma (S.K.); a.bah@um5r.ac.ma (A.B.); o.ansari@um5r.ac.ma (O.A.); rabab_elattar@um5.ac.ma (R.E.A.); oumayma_cherqi@um5.ac.ma (O.C.)

* Correspondence: abdessamad.idouanaou@um5r.ac.ma; Tel.: +212-606013758

Abstract

This study investigates the potential of bio-based phase change materials (bio-PCMs) to reduce both operational and embodied carbon in Moroccan service buildings. Using EnergyPlus 8.3 simulations and life cycle assessment (LCA), the research evaluates the integration of five bio-PCM types across six Moroccan climate zones. Results show that climate-specific PCMs can lower heating and cooling energy demands by up to 20.3% and 28.0%, respectively, leading to operational CO_2 emission reductions between 17.0% and 24.0%. Bio-PCM Q25 performed best in Coastal, Mediterranean, and Saharan zones, Q23 in Continental and Mountainous areas, and Q29 in hot-arid climates. In parallel, bio-based PCM M27 exhibited an embodied carbon of only 0.08 $kgCO_2/kg$ over 97% lower than conventional PCMs like paraffin or stearic acid. These findings confirm that optimized bio-PCM integration, combined with passive design strategies, offers a robust solution to decarbonize buildings in hot and diverse climates like Morocco. The study provides practical guidelines for material selection and policy direction toward climate-adapted, low-carbon construction.

Keywords: bio-PCM; embodied carbon; energy simulation; life cycle assessment; thermal storage; Moroccan climate

check for updates

Academic Editor: Antonio Caggiano

Received: 1 September 2025
Revised: 29 September 2025
Accepted: 4 October 2025
Published: 16 October 2025

Citation: Idouanaou, A.; Malha, M.; Kardellass, S.; Bah, A.; Ansari, O.; El Attar, R.; Cherqi, O. Integrated Evaluation of Bio-Based Phase Change Materials to Reduce Operational and Embodied Carbon in Service Buildings Across Multiple Climate Zones. *Buildings* **2025**, *15*, 3720. https://doi.org/10.3390/buildings15203720

Copyright: © 2025 by the authors. Licensee MDPI, Basel, Switzerland. This article is an open access article distributed under the terms and conditions of the Creative Commons Attribution (CC BY) license (https://creativecommons.org/licenses/by/4.0/).

1. Introduction

The building sector is a major contributor to global greenhouse gas emissions due to both operational energy consumption and embodied carbon from construction materials [1,2]. In Morocco, the rapid expansion of service buildings such as offices, hotels, and public facilities has led to a substantial increase in energy demand, particularly for heating and cooling, given the country's diverse and contrasting climate [3,4]. This dual carbon challenge requires innovative approaches that address both operational and embodied emissions simultaneously.

One emerging strategy involves the use of bio-based phase change materials (bio-PCMs) [5]. These materials, derived from renewable organic sources such as vegetable oils, fatty acids, and natural waxes, store and release thermal energy by exploiting latent heat during phase transitions [6,7]. By integrating bio-PCMs into the building envelope (walls, floors, ceilings), it becomes possible to enhance thermal inertia, reduce peak heating and

cooling loads, and consequently lower electricity consumption [8,9]. At the same time, the renewable and low-impact nature of these materials can significantly reduce embodied carbon compared to conventional petrochemical-based PCMs [10]. Unlike most previous studies that separately assess either the energy performance or the environmental impacts, this research adopts an integrated and novel methodology combining detailed dynamic energy simulations and comprehensive life cycle assessment (LCA). This innovative approach enables the simultaneous evaluation of both operational energy performance and embodied carbon impacts, specifically tailored to Morocco's diverse climatic conditions, representing a significant methodological advancement in the field.

In the Moroccan context, where summer temperatures can exceed 45 °C in hot inland regions and winters can be cold in mountainous areas, passive thermal regulation strategies like PCMs are particularly relevant [11,12]. Despite their potential, there is limited research evaluating the combined impact of bio-PCMs on both energy efficiency and lifecycle carbon emissions in service buildings. This study aims to fill this gap by assessing the dual benefits of bio-PCM integration in the Moroccan climate.

1.1. Literature Review

Numerous investigations report that incorporating bio-based PCMs in walls can significantly reduce indoor heat gains and smooth temperature fluctuations. For instance, Kosny et al. experimentally studied a wood-framed wall with PCM-enhanced fiber insulation and found that peak-hour heat gains were reduced by 21–37% across climates [13]. In a similar simulation study, Anter et al. showed that embedding layers of lauric acid PCM (RT35HC) on both inner and outer wall faces lowered the wall's average interior temperature from 31.1 °C to 27.7 °C and reduced total summer heat gain by 66% [14]. Guermat et al. modeled a bio-PCM (beeswax/vegetable oil blend) layer in brick walls for various Algerian cities and observed that the PCM decreased the peak indoor surface temperature by about 3.0–3.9 °C depending on the climate [15]. These examples illustrate that bio-PCMs can act as "thermal buffers," absorbing heat during hot periods and releasing it later, thus cutting peak thermal loads. The magnitude of performance improvement depends strongly on PCM placement and quantity. Both modeling and experiments have confirmed that there is an optimal location for the PCM layer within the wall. Jin et al. found experimentally that placing a PCM layer at one-fifth of the wall thickness (near the indoor side) yielded the best result, reducing the peak heat flux through the wall by roughly 40–41% compared to a non-PCM wall [16]. In practice, increasing the PCM thickness also enhances effect: Guermat et al. showed that going from 1 cm to 3 cm of bio-PCM layer further diminished interior temperature swings (from ~5 °C to ~1.1 °C amplitude) and flux variations [15]. Overall, the literature agrees that carefully optimized bio-PCM layers can significantly improve wall thermal performance, effectively acting as dynamic insulation to enhance building energy efficiency.

Bio-based PCMs offer environmental benefits that align with green-building objectives. Since many conventional PCMs (e.g., paraffins) are petroleum-derived, replacing them with renewable alternatives can reduce embodied carbon. Benhorma et al. note that bio-PCM can utilize agricultural or industrial byproducts (such as coconut oil, beeswax, animal fats, or biomass-derived compounds) to meet sustainability goals [7]. These natural materials are generally non-toxic and biodegradable, making leakage or disposal less problematic than synthetic options. For example, coconut fat and plant oils have been successfully recycled into PCMs for TES. However, bio-PCMs also pose unique challenges. The same review highlights potential drawbacks such as susceptibility to microbial degradation and changes in thermal/chemical stability over time. Long-term cycling tests are thus important. Notably, some studies report good durability: for instance, Öztürk et al. demonstrated

that a micro-encapsulated PCM/wood-fiber panel retained its heat storage capacity after 600 melt–freeze cycles [17]. Overall, the shift to bio-derived PCMs is seen as a promising route toward more sustainable building TES, provided issues of longevity and compatibility are addressed.

Various methods have been developed to incorporate bio-PCMs into building materials. One common approach is direct impregnation/immersion into porous or fibrous matrices. Boussaba et al., for example, soaked a clay–cellulose fiber composite in molten coconut fat, yielding a stable composite with 56 wt% PCM loading and no leakage [18]. The resulting panel could then be sandwiched in wall assemblies as a latent heat storage element. Similarly, micro-encapsulation techniques encapsulate bio-PCM droplets in polymer shells, which are then embedded into construction materials. Öztürk et al. produced microcapsules of a fatty PCM and mixed them into a wood fiber–starch composite; the SEM images confirmed uniformly distributed intact PCM capsules [17]. This micro PCM/wood composite demonstrated low thermal conductivity (0.1041 W/m·K) and preserved its latent-heat function over hundreds of cycles. Another strategy is to use PCM thermal shields or panels. Jin et al. used sealed "PCM thermal shield" layers (flat PE bubbles filled with PCM) inserted at different depths in insulated walls. Through dynamic wall tests, they showed that placing the shield at 1/5 of the insulation thickness maximized performance (∼41% reduction in peak flux) [19]. In general, these works underscore that integration method (e.g., macro vs. micro encapsulation), as well as layer placement and geometry, critically influence the thermal outcomes. The literature suggests preferring simple, low-cost processes (like immersion or composite casting) for bio composites, while tailoring layer design to the building's climate context.

The results of this study will provide practical recommendations directly applicable by Moroccan engineers, architects, and policymakers. By offering concrete, optimized solutions for integrating bio-PCMs tailored to local climatic conditions, this research supports informed decision-making toward sustainable construction, aligning with Morocco's national goals of reducing carbon emissions and improving the energy efficiency of the building sector.

1.2. Goals and Objectives

The primary goal of this study is to evaluate how the integration of bio-based phase change materials (bio-PCMs) in Moroccan service buildings can reduce the overall carbon footprint both operational and embodied. The specific objectives are as follows:

- Quantify the reduction in electricity demand resulting from the use of Bio-PCMs through dynamic energy simulations comparing scenarios with and without PCM integration under representative Moroccan climate conditions.
- Assess the embodied carbon footprint of Bio-PCM by conducting life cycle assessments (LCA) of different envelope components using bio-based and synthetic Bio-PCMs, to determine their carbon impact from the construction phase.
- Compare material solutions by identifying the most effective Bio-PCMs offering the best trade-off between thermal storage capacity and low embodied carbon, and recommending their optimal applications (roof, floor, walls, etc.).
- Provide design recommendations for Morocco's service building sector based on the simulation and LCA results, taking into account the country's specific climatic characteristics (e.g., intense summer heat, cool nights) and constraints related to cost and material availability.

By addressing these objectives, this research aims to demonstrate that the strategic use of bio-based PCMs can support the transition toward more sustainable buildings in

Morocco by enhancing energy performance and reducing both operational and embodied carbon emissions.

2. Materials and Methods

2.1. Climatic Zoning and Meteorological Inputs

Morocco exhibits a wide diversity of climatic conditions that significantly influence building energy dynamics and the carbon footprint associated with operational energy use [20]. To capture this variability, the country is divided into six representative climatic zones, each characterized by distinct thermal patterns and meteorological phenomena Figure 1.

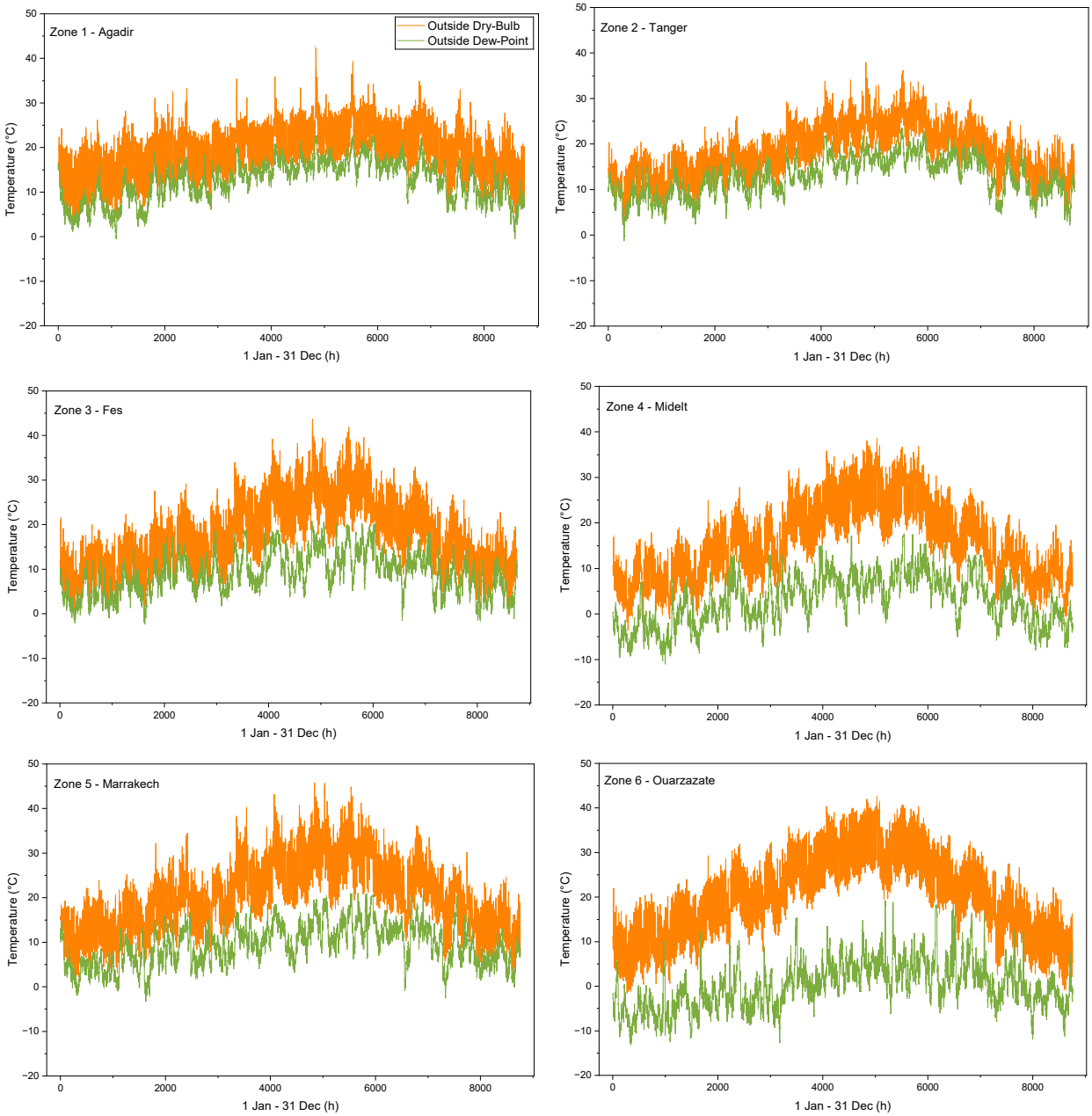


Figure 1. Year-round outdoor temperature profiles for Morocco's six climatic zones.

Zone 1 (Coastal & Desert, e.g., Agadir, Laayoune) features a mild, humid climate with moderate annual temperature variation, where oceanic winds enhance natural ventilation and convective heat transfer. Zone 2 (Mediterranean, e.g., Tangier, Oujda) experiences

cool, wet winters and hot, dry summers, with sea breezes helping to moderate outdoor temperatures and reduce cooling loads. Zone 3 (Continental, e.g., Fès, Meknès) is marked by strong seasonal temperature swings, generating both heating and cooling demands. Zone 4 (Semi-Arid Mountainous, e.g., Midelt, Atlas Mountains) exhibits cold winters, warm summers, and high solar radiation due to elevation. Zone 5 (Hot Arid, e.g., Marrakech) undergoes extremely high summer temperatures, strong diurnal variation, and very low rainfall. Zone 6 (Saharan, e.g., Ouarzazate) is characterized by intense solar radiation, dry and hot daytime conditions, and sharp nocturnal cooling [20].

Hourly meteorological data including dry-bulb temperature, dew-point temperature, solar radiation, and wind speed were generated using Meteonorm 8.0, a validated stochastic weather data tool [3,21]. These climate inputs were used to simulate the thermal behavior of service buildings over a complete year (1 Jan–31 Dec) with hourly resolution (8760 h). As shown in Figure 1, significant inter-zonal variations in temperature profiles directly influence heating and cooling demands. These climatic patterns are critical in evaluating the effectiveness of bio-based PCMs in reducing operational energy use and associated CO_2 emissions.

2.2. Building Description and Materials

The reference service building modeled in this study represents a single-story generic office space, typical of Moroccan public administration facilities. The design incorporates large glazed openings covering approximately 40% of the façade area, strategically distributed to enhance daylight penetration into occupied zones, as shown in Figure 2. The building includes a conditioned floor area of 399.7 m^2 and a conditioned volume of 1398.8 m^3, with the zone multiplier set to 1. It is assumed to operate at full occupancy, with an occupant density of 0.1110 people/m^2, and the occupancy and HVAC schedules reflect standard working hours, as defined in Table 4 of the study by Idouanaou et al. (2025) [3].

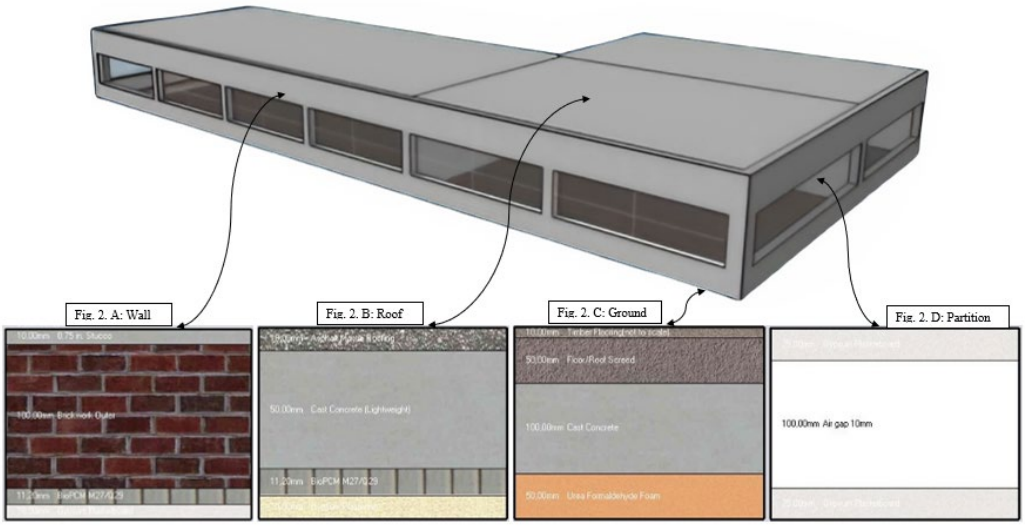


Figure 2. Geometric model of the simulated single-story service building.

The construction system of the reference service building reflects common materials used in Moroccan service buildings. Each component is characterized by its internal heat capacity, thermal resistance, and U-value, as summarized in Table 1. All thermal transmittance values (U-values) were calculated following BS EN ISO 6946, accounting for thermal bridging [22]. All building surfaces (walls and roof) are assumed to be thermally conditioned and occupied, with no unconditioned or unoccupied volumes. The building envelope assemblies used in this study are consistent across all scenarios to ensure that only the bio-PCM integration strategy varies. This standardization isolates the thermal

and carbon impact of PCM types. The bio-PCM is integrated exclusively in the roof and external wall assemblies.

Table 1. Physical and thermal characteristics of building envelope components.

Component	Physical and Thermal Characteristics	Layer Composition (Outside to Inside)
Wall	The external wall exhibits a moderate internal heat capacity of 121.35 kJ/m^2·K and a U-value of 2.548 W/m^2·K, corresponding to a low-insulated masonry construction. This baseline configuration serves to evaluate the potential benefits of bio-PCM integration for envelope enhancement.	Figure 2A: Wall
Roof	The roof has the lowest heat storage capacity (38.47 kJ/m^2·K) and the highest U-value (2.768 W/m^2·K) among the envelope components, making it highly sensitive to solar radiation gains. This component is of particular interest for PCM application due to its thermal exposure.	Figure 2B: Roof
Partition	The internal partition walls, with an internal heat capacity of 22.50 kJ/m^2·K and a U-value of 1.639 W/m^2·K, contribute to internal thermal zoning but are not directly exposed to outdoor temperature variations.	Figure 2D: Partition
Ground	The ground floor presents the highest internal heat capacity (138.20 kJ/m^2·K) and the lowest U-value (0.574 W/m^2·K), providing strong thermal inertia and acting as a stabilizing mass against diurnal temperature fluctuations.	Figure 2C: Ground

In all simulation scenarios, the window configuration was kept constant to isolate the impact of the envelope's thermal mass and bio-PCM integration. The building façade features double-glazed windows representing 40% window-to-wall ratio, with a standard height of 1.5 m and sill height of 0.80 m. The glazing system is composed of two 6 mm glass panes (outer: Generic REF A CLEAR MID 6 MM, inner: Generic CLEAR 6 MM) separated by a 6 mm air gap. The overall U-value is 2.824 W/m^2·K, with a solar heat gain coefficient (SHGC) of 0.201 and light transmission of 12.7%, indicating a moderate solar control capacity. To mitigate solar heat gains, all windows are equipped with internal blinds using high-reflectivity slats, which activate based on indoor air temperature control (setpoint 24 °C), following the custom occupancy schedule according to the configuration detailed in Table 4 of the study conducted by Idouanaou et al. (2025) [3]. This fixed window and shading configuration ensures thermal performance consistency across all PCM comparison scenarios.

All scenarios, including the reference and Bio-PCM-enhanced cases, use the same HVAC system to ensure consistent comparison. The building is equipped with a Variable Refrigerant Flow (VRF) system with heat recovery, combined with a Dedicated Outdoor Air System (DOAS) for ventilation. Heating and cooling are controlled by setpoints of 20 °C and 24 °C, with setback temperatures of 12 °C and 28 °C, respectively. Natural ventilation is also activated when indoor air remains above 22 °C to enable free cooling. Mechanical ventilation is defined by a fresh air rate of 4 L/s per person plus an area-based component. The seasonal coefficient of performance (CoP) is set to 2.5 for heating and 3.0 for cooling. HVAC control schedules were adopted from Table 4 of Idouanaou et al. (2025) [3] and applied uniformly across all scenarios. As the entire system operates on electricity, it represents the main contributor to operational CO_2 emissions, which are calculated using Moroccan grid-specific emission factors [23].

2.3. Bio-PCM Scenarios and Reference Configuration

To assess the contribution of bio-based phase change materials (Bio-PCMs) to energy performance and carbon reduction, five distinct Bio-PCM integration scenarios were developed and compared against a non-PCM reference building. The reference model

shares the same geometry, occupancy, HVAC settings, glazing characteristics, and envelope construction as the PCM-enhanced models, ensuring consistent baseline conditions.

In all scenarios, the Bio-PCM layer was integrated within the wall construction and simulated using the enthalpy–temperature method available in EnergyPlus. This modeling approach allows for an accurate representation of the latent heat exchange during the material's phase transitions. The five scenarios differ by the type of Bio-PCM used, each defined by its unique enthalpy–temperature response curve and melting range, as shown in Figure 3. These formulations (Bio-PCM M27-Q21, Q23, Q25, Q27, and Q29) were selected to span a temperature range between 21 °C and 29 °C, which corresponds to typical comfort temperatures in Moroccan service buildings.

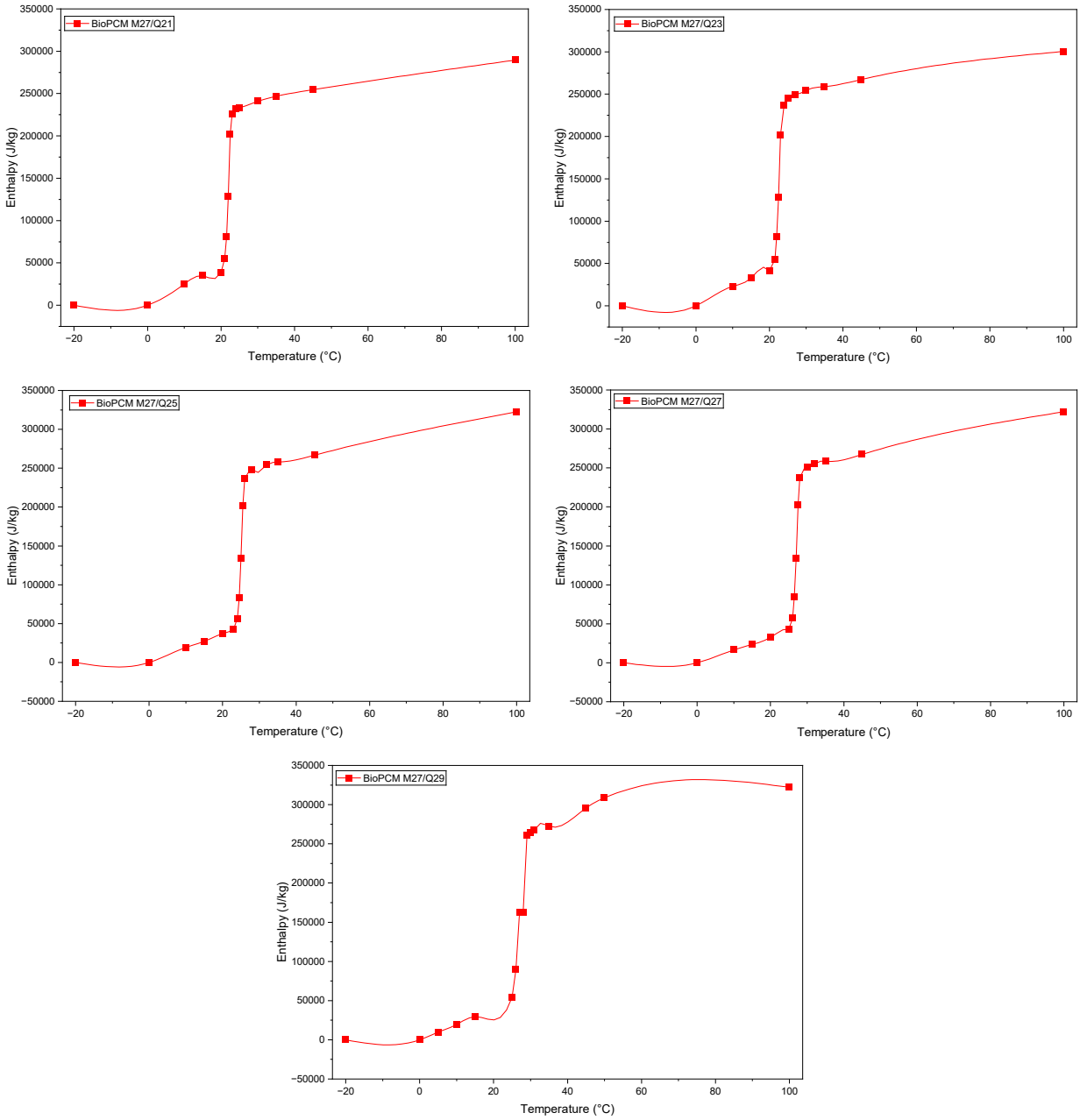


Figure 3. Enthalpy–temperature curves of the five Bio-PCM formulations used in the simulation scenarios.

The same material configuration was applied across all PCM scenarios to ensure uniform comparison conditions. The Bio-PCM layer has a fixed thickness and composition,

and its thermophysical and environmental characteristics are presented in Table 2. These properties reflect experimentally measured data and embodied carbon values sourced from the ICE v1.6 database [24]. The PCM layer thickness was set to 0.0112 m, corresponding to the standard sheet thickness provided by the material manufacturer. While greater storage capacity can be obtained by applying double or triple layers in real applications, the thickness was fixed in this study to focus on the comparative effect of different bio-PCM formulations.

Table 2. Thermophysical and environmental properties of the Bio-PCM layer used in all scenarios.

Component	Bio-PCM Property	Value	3D Model
Wall/Roof	Thermal conductivity Specific heat capacity Density Layer thickness Embodied carbon	0.200 (W/m·K) 1970 (J/kg·K) 235 (kg/m^3) 0.0112 (m) 0.08 (kgCO_2e/kg)	

This standardization of material parameters ensures that any observed differences in energy savings or carbon impacts are attributable to the PCM's thermal activation characteristics rather than to changes in physical properties or construction methods. It is important to note that the life cycle assessment (LCA) in this study focuses solely on the embodied carbon of PCM rather than a full cradle-to-grave building analysis.

The embodied carbon values reported for bio- and conventional PCMs in this study are limited to the production stage (cradle-to-gate) as obtained from the ICE v1.6 database. Transportation, installation, and end-of-life disposal impacts were excluded to ensure a consistent comparison framework between PCM types. These additional life cycle stages are acknowledged as important but are left for future work.

2.4. Mathematical Formulation of the Energy Model

2.4.1. Surface Convection

To improve simulation accuracy, adaptive convection algorithms were applied to both interior and exterior surfaces [25]. These algorithms automatically adjust the convective heat transfer coefficients based on surface orientation, temperature gradients, and airflow conditions [26]. For interior surfaces, the model selects appropriate correlations depending on whether the surface is a wall, ceiling, or floor [27]. For exterior surfaces, wind speed, surface roughness, and tilt are considered [28]. This approach ensures a more realistic and responsive representation of heat exchange between surfaces and air, as recommended in the EnergyPlus documentation.

2.4.2. Conduction Finite Difference

The thermal performance of multilayer building envelopes was simulated using the Conduction Finite Difference (CondFD) model implemented in EnergyPlus [29]. This method discretizes the one-dimensional heat conduction equation through the material layers and applies a semi-implicit Crank–Nicolson scheme, with the possibility to incorporate temperature-dependent properties and phase change effects [30]. The transient heat conduction is governed by an energy balance at each node. The Crank–Nicolson scheme provides a second-order time-accurate solution. The discretized form at node i is expressed as shown in Equation (1):

$$C_P \rho \Delta_x \frac{T_i^{j+1} - T_i^j}{\Delta t} = \frac{1}{2}\left[k_\omega\left(\frac{T_{i+1}^{j+1} - T_i^{j+1}}{\Delta x} + \frac{T_{i+1}^j - T_i^j}{\Delta x}\right) + k_E\left(\frac{T_{i-1}^{j+1} - T_i^{j+1}}{\Delta x} + \frac{T_{i-1}^j - T_i^j}{\Delta x}\right)\right] \quad (1)$$

when a fully implicit scheme is preferred, a simplified first-order Adams–Moulton form is used instead, as given in Equation (2):

$$C_P \rho \Delta_x \frac{T_i^{j+1} - T_i^j}{\Delta t} = k_\omega\left(\frac{T_{i+1}^{j+1} - T_i^{j+1}}{\Delta x}\right) + k_E\left(\frac{T_{i-1}^{j+1} - T_i^{j+1}}{\Delta x}\right) \quad (2)$$

The thermal conductivity of each node is updated dynamically with temperature, using a linear relation as shown in Equation (3):

$$k_i = k_0 + k_1(T_i - 20) \quad (3)$$

The thermal conductivity between two adjacent nodes is calculated by linear interpolation, as shown in Equation (4):

$$k_\omega = \frac{k_i^{j+1} + k_{i+1}^{j+1}}{2},\ k_E = \frac{k_i^{j+1} + k_{i-1}^{j+1}}{2} \quad (4)$$

For phase-change materials (PCMs), the model uses an enthalpy–temperature function to describe latent heat phenomena, as expressed in Equation (5):

$$h_i = HTF(T_i) \quad (5)$$

In this case, the apparent heat capacity C_P is derived from the slope of the enthalpy function *HTF*. Once the temperature field has been calculated, the heat flux at the inside surface node is defined directly, as shown in Equation (6):

$$Q_{Dreport,1} = Q_{inside} \quad (6)$$

For internal nodes, the heat flux is updated iteratively using a node-by-node energy balance that accounts for internal source terms and nodal thermal inertia, as presented in Equation (7):

$$Q_{Dreport,i} = Q_{Dreport,i+1} + HeatCap_{\ 1}\frac{T_{i+1}^{new} - T_{i+1}^{old}}{\Delta t} - Q_{source,i} + HeatCap_{\ 2}\frac{T_i^{new} - T_i^{old}}{\Delta t} \quad (7)$$

Here, the heat capacitance of a half-node is computed using the expression in Equation (8):

$$HeatCap_{\ n} = C_P \rho \Delta_x \cdot \frac{1}{2} \quad (8)$$

This approach enables the detailed temporal and spatial tracking of conductive heat transfer and energy storage within each construction layer.

In this study, the thermal behavior of a bio-based PCM layer was modeled using the enthalpy–temperature method Equation (5), allowing accurate tracking of latent heat during melting and solidification phases [30]. The PCM properties (e.g., melting range, latent heat, specific heat) were derived from experimental bio-sourced materials.

2.4.3. Heat Pump Systems

The energy performance of the Variable Refrigerant Flow (VRF) heat pump system was modeled using a set of empirical functions that modify the rated Energy Input Ratio (*EIR*) according to the part-load ratio (*PLR*), ambient temperatures, and operating conditions [31].

These functions allow the system to reflect realistic efficiency variations in both heating and cooling modes using a unified mathematical formulation.

To account for the variation in system efficiency under part-load operation, a third-order polynomial function is applied when the part-load ratio is less than or equal to 1, as shown in Equation (9):

$$EIRFPLR = a + b \cdot PLR + c \cdot PLR^2 + d \cdot PLR^3 \tag{9}$$

For overload conditions, where the load exceeds the rated capacity ($PLR > 1$), a separate polynomial is used, as shown in Equation (10):

$$EIRFPLR = e + f \cdot PLR + g \cdot PLR^2 + h \cdot PLR^3 \tag{10}$$

These correction factors adjust the energy input based on the deviation from ideal part-load conditions.

The total electrical power consumed by the VRF system is calculated by multiplying the rated thermal capacity with all relevant correction factors, as shown in Equation (11):

$$Power = \left(\frac{\dot{Q}_{rated} \cdot CAPFT}{COP_{ref}} \right) \cdot EIRFT \cdot EIRFPLR \cdot HPRTF \cdot EIR_{deforst} \tag{11}$$

This expression integrates the effects of part-load, temperature, runtime, and defrost penalties.

The coefficient of performance (*COP*) is obtained by dividing the useful thermal output by the total electrical input, including auxiliary loads, as shown in Equation (12):

$$COP = \frac{\dot{Q}_{deliverd}}{Power + P_{crankcase} + P_{evap \cdot pump} + P_{defrost}} \tag{12}$$

This indicator reflects the real efficiency of the system, including all parasitic losses. In heat recovery (*HR*) mode, an additional polynomial modifier is applied to account for altered system behavior due to simultaneous heating and cooling demands. The correction is given in Equation (13):

$$HREIRMod = a + b \cdot T_{ent} + c \cdot T_{ent}^2 + d \cdot T_{cond} + e \cdot T_{cond}^2 + f \cdot T_{ent} \cdot T_{cond} \tag{13}$$

The modified power consumption under *HR* mode is then computed as shown in Equation (14):

$$Power_{HR} = Power \cdot HREIRMod \tag{14}$$

Finally, a transient function models the gradual transition of power when the system switches into *HR* mode, as shown in Equation (15):

$$Power(t) = k_{EIR} \cdot Power_{HR} + (1 - k_{EIR}) \cdot Power_{HR} \cdot \left(1 - e^{-t/\tau EIR}\right) \tag{15}$$

This formulation captures the system's dynamic response during control mode changes. Although the same mathematical structure is used for both heating and cooling modes, the difference lies in the performance coefficients, operating limits, and sensitivity to ambient conditions. Cooling mode is more affected by high outdoor temperatures, while heating mode performance degrades at low ambient conditions and may require defrosting [31]. Therefore, the coefficients in the correction curves (e.g., a to h) are mode-specific and calibrated separately for heating and cooling operation.

2.4.4. CO_2 Emissions

The HVAC system consists of a Variable Refrigerant Flow (VRF) air-cooled system with heat recovery and a Dedicated Outdoor Air System (DOAS) to ensure efficient heating, cooling, and ventilation [32]. In EnergyPlus, CO_2 emissions from electricity consumption are calculated using a CO_2 emission factor specific to the electricity source. This factor, expressed in kilograms of CO_2 per kilowatt-hour ($kgCO_2/kWh$), depends on the energy mix used for electricity generation (e.g., coal, natural gas, or renewables) [33]. By reducing heating and cooling loads through the thermal buffering effect of the bio-PCM, the integrated solution contributes to lowering the annual CO_2 emissions, as quantified using the national grid emission factor [23].

2.5. Validation of the Simulation Approach

To ensure the reliability of the simulation results, a comparative validation was conducted using the reference data reported by Hamdaoui et al. [34]. The study employed comparable building typologies and climatic zones, enabling a consistent benchmarking framework. The baseline simulation in this study (No PCM, ACH 3, WWR 40%) was compared to two validated scenarios from Hamdaoui et al. [34]: one with ACH 0.6 and WWR 25%, and another with ACH 0.6 and WWR 35%.

As shown in Figure 4, the heating electricity demands predicted in the reference simulation closely match the trend observed in Hamdaoui et al.'s configurations, especially in Zones 1 to 3, with discrepancies attributed mainly to differences in airtightness (ACH) and window to wall ratio (WWR). In particular, higher WWR and infiltration rates in the reference case led to increased heat losses, especially in colder zones (e.g., Zone 4), confirming the model's sensitivity to envelope and ventilation parameters.

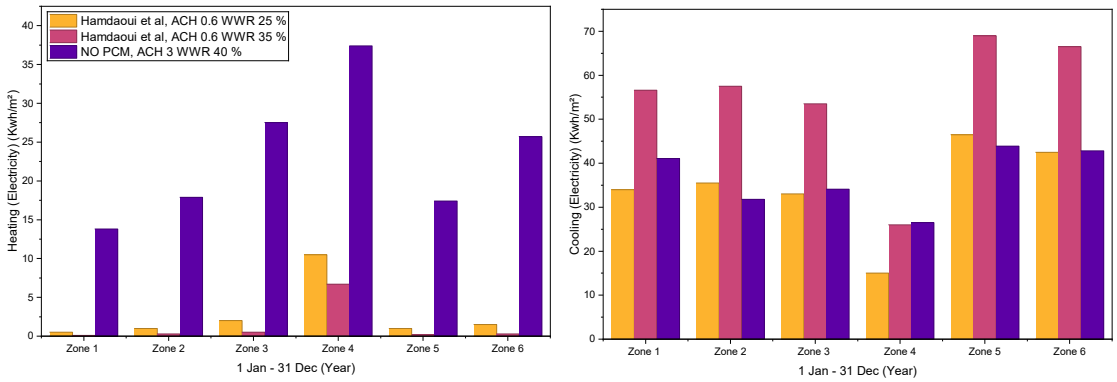


Figure 4. Annual heating and cooling demand comparison for model validation [34].

For cooling electricity demands, the reference model also followed a comparable trend, although higher values were observed in Zones 5 and 6 due to increased solar gains and internal heat retention associated with the higher WWR. These deviations are consistent with the physical behavior of envelope thermal balance and validate the accuracy of the simulation assumptions.

Overall, the alignment of energy demand trends across multiple climate zones supports the validity of the simulation model and reinforces its applicability in assessing the thermal and carbon impacts of bio-PCM integration strategies.

3. Results

3.1. Impact of Bio-PCM Integration on Heating Energy Demand

The integration of Bio-PCM Q21 into the building envelope led to a noticeable reduction in annual heating energy demand across all six Moroccan climatic zones. Compared

to the reference building without PCM, the Bio-PCM-enhanced configuration achieved significant savings, confirming the effectiveness of thermal energy storage in stabilizing indoor temperatures during cold periods, as shown in Figure 5.

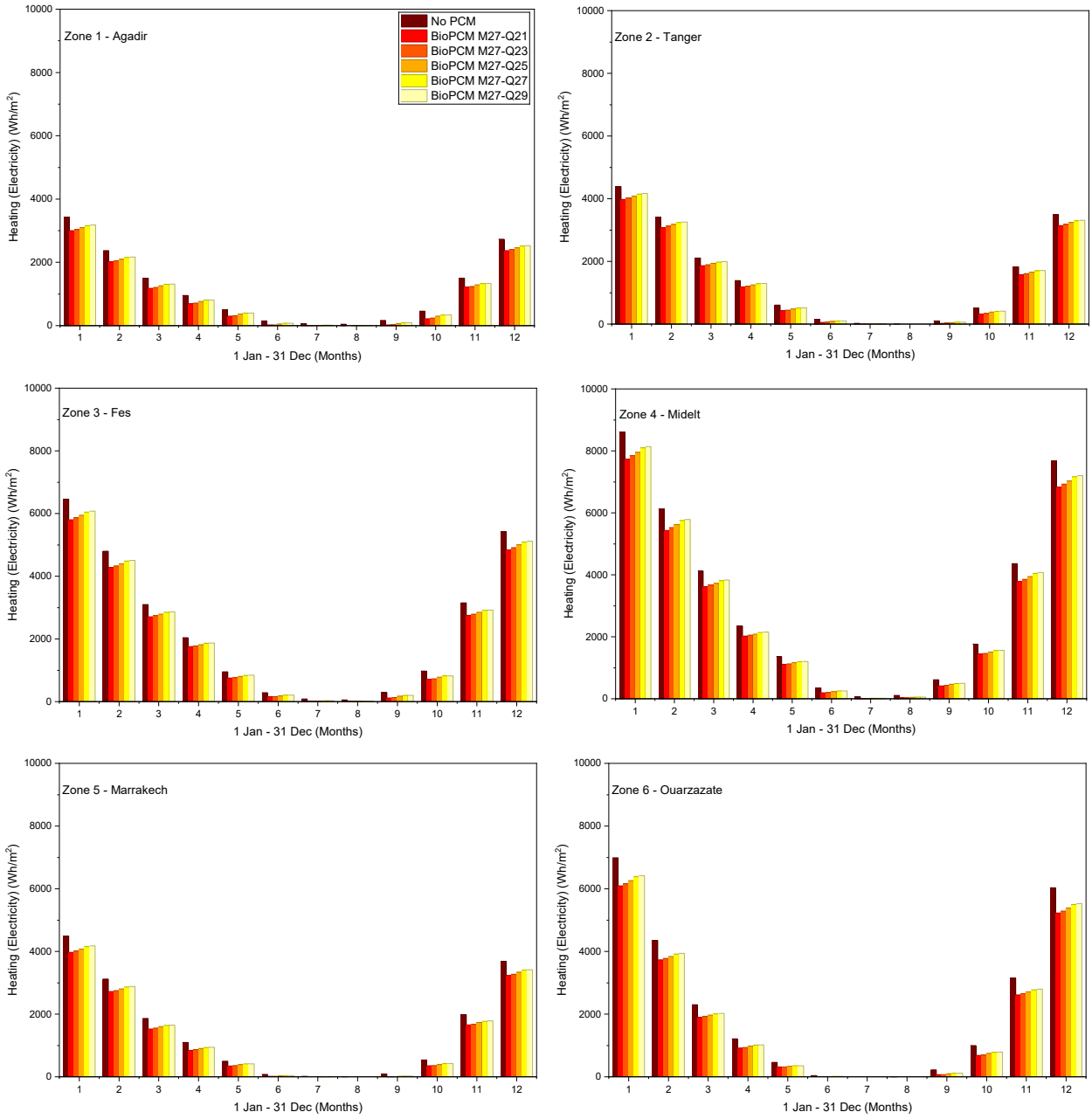


Figure 5. Monthly heating demand reduction for different Bio-PCM types across Moroccan cities.

In Zone 1, the annual heating demand dropped from 13.8 kWh/m^2·year to 11 kWh/m^2·year, representing a reduction of approximately 20.3%. Zone 2 experienced a decrease from 17.9 to 15.6 kWh/m^2·year, yielding a 12.9% reduction. Similarly, in Zone 3, the demand decreased from 27.5 to 23.8 kWh/m^2·year, corresponding to a 13.5% reduction. In the colder Zone 4, where heating needs are highest, Bio-PCM Q21 still achieved a notable saving of 12.8%, reducing the energy demand from 37.4 to 32.6 kWh/m^2·year. For Zone 5, characterized by hot-arid conditions, the heating load decreased from 17.4 to 14.6 kWh/m^2·year, equivalent to a 16.1% reduction. Finally, in Zone 6, the demand was reduced from 25.7 to 21.5 kWh/m^2·year, reflecting a 16.3% improvement.

These results demonstrate the consistent performance of Bio-PCM Q21 in reducing heating loads across diverse climates. The observed reductions, ranging between 12.8% and 20.3%, highlight the ability of this material to store solar heat during the day and release it during night hours, thereby mitigating heating needs. As such, Bio-PCM Q21 presents a compelling passive solution for lowering energy consumption in Moroccan service buildings, especially when integrated into roofs and external walls exposed to significant thermal fluctuations.

3.2. Impact of Bio-PCM Integration on Cooling Energy Demand

The integration of Bio-PCM Q29 into the building envelope demonstrated substantial effectiveness in reducing cooling energy demand across all Moroccan climatic zones, especially during peak summer periods as illustrated in Figure 6. This performance is attributed to the high latent heat storage capacity of the Q29 formulation, whose melting range (centered around 29 °C) aligns well with typical indoor comfort temperatures in hot climates.

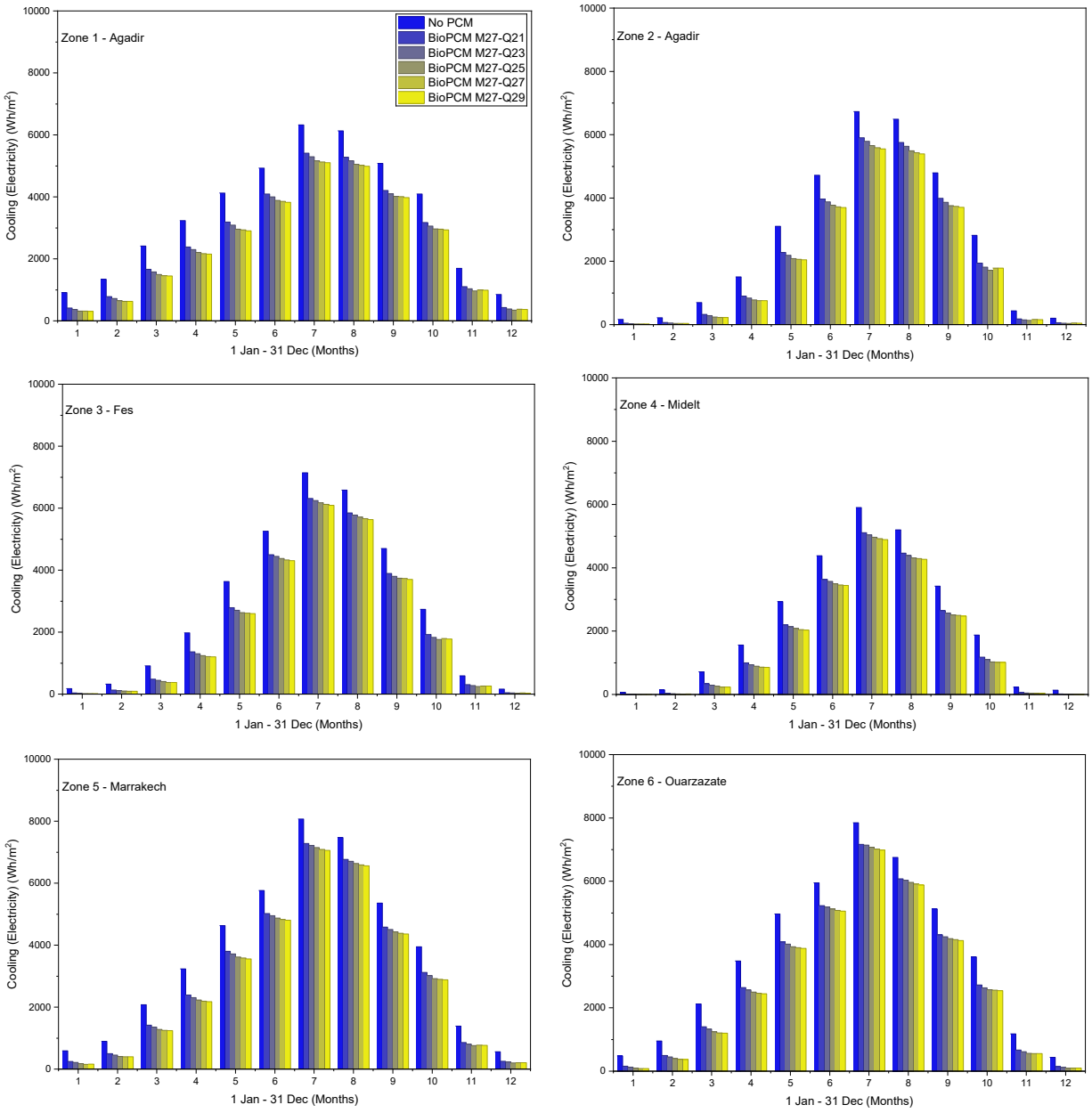


Figure 6. Monthly cooling demand profiles for various Bio-PCM types in Moroccan climatic zones.

In Zone 1, the annual cooling demand dropped from 41.1 to 29.6 kWh/m^2·year, representing a notable 28.0% reduction. In Zone 2, cooling energy consumption decreased from 31.8 to 23.4 kWh/m^2·year (26.4% savings), while in Zone 3, the reduction reached 23.8%, with demand falling from 34.1 to 26.0 kWh/m^2·year. Zone 4, characterized by relatively milder summer conditions, experienced a drop from 26.5 to 19.2 kWh/m^2·year, equating to a 27.5% decrease. In hotter climates such as Zone 5, Bio-PCM Q29 reduced cooling demand from 43.9 to 34.1 kWh/m^2·year, resulting in a 22.3% reduction. Similarly, Zone 6 showed a decline from 42.8 to 33.2 kWh/m^2·year, equivalent to a 22.4% reduction.

These results indicate that Bio-PCM Q29 is especially well-suited for cooling-dominated zones, offering consistent energy savings of 22–28% depending on the climate. This is primarily due to the material's ability to absorb excess indoor heat during daytime hours and release it during cooler night periods, thus dampening peak cooling loads. As illustrated in Figure 6, the monthly cooling profiles clearly show a shift in load patterns and a significant attenuation of cooling peaks during the summer months when the PCM is most active.

The findings confirm the potential of Bio-PCM Q29 as a high-performance passive cooling strategy, especially in hot and arid Moroccan zones where solar gains and internal heat accumulation are dominant. Its application contributes not only to electricity savings but also to reducing stress on HVAC systems and improving indoor thermal comfort during extreme heat events.

3.3. Impact of Bio-PCM on Operational Carbon Emissions

The integration of Bio-PCMs into the building envelope not only reduces energy demand for heating and cooling but also translates into significant reductions in operational carbon emissions due to Morocco's electricity generation mix. Since all HVAC systems in the model operate on grid electricity, the CO_2 emissions are directly proportional to electricity consumption as illustrated in Figure 7. The results confirm that Bio-PCMs contribute meaningfully to emission mitigation across all six climatic zones, with reductions ranging from 19% to 24%.

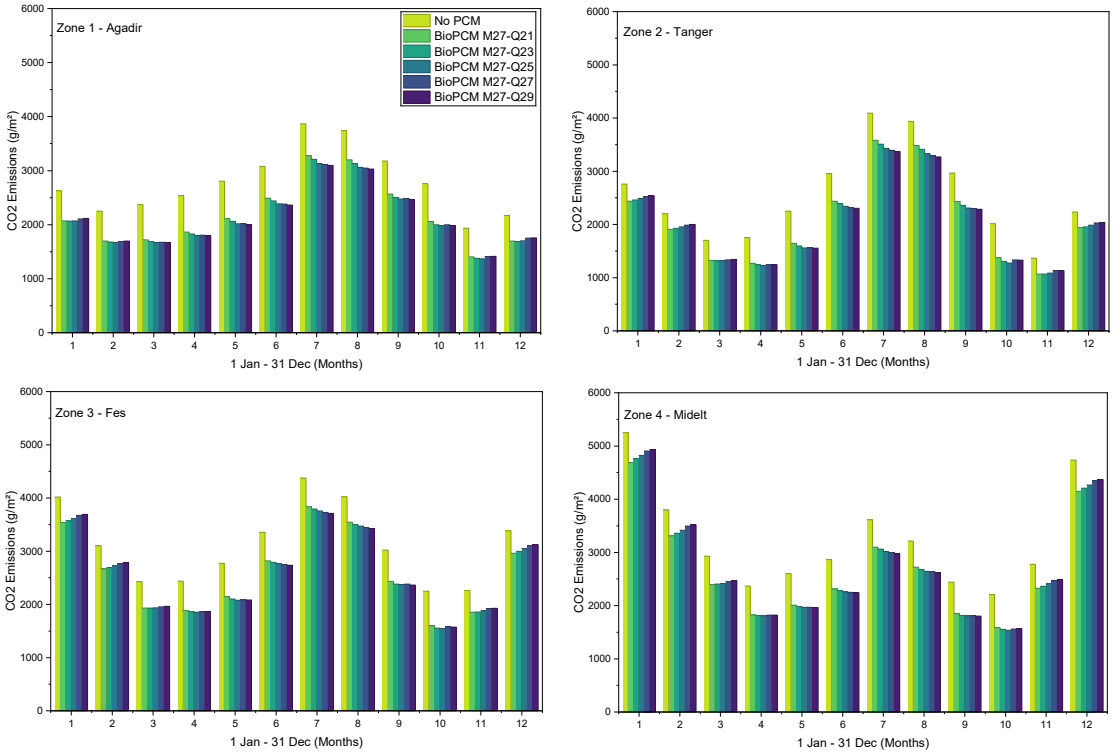


Figure 7. *Cont.*

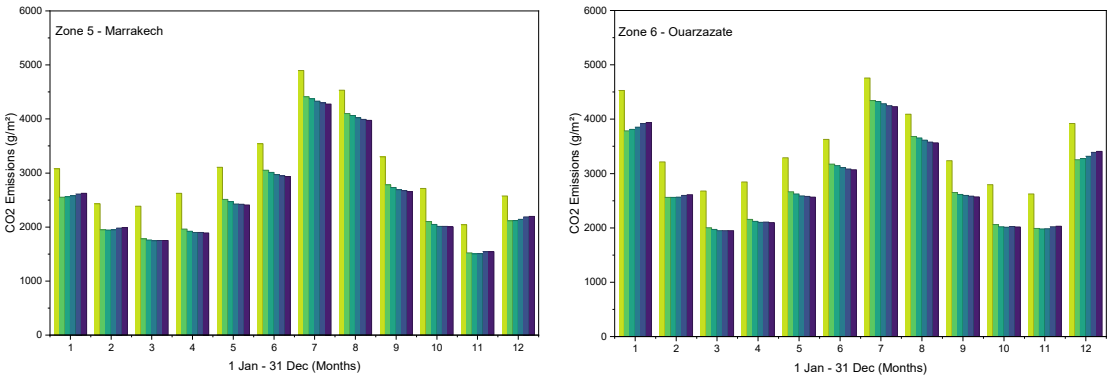


Figure 7. Comparison of annual CO_2 emissions across Bio-PCM types and climatic zones for various Moroccan cities.

In Zone 1, where Bio-PCM Q25 was used, operational carbon emissions decreased from 33.3 $kgCO_2/m^2$·year to 25.3 $kgCO_2/m^2$·year, representing a 24.0% reduction. In Zone 2, the same PCM formulation (Q25) reduced emissions by 19.5%, from 30.2 to 24.3 $kgCO_2/m^2$·year. For Zone 3, Bio-PCM Q23 led to a decrease from 37.4 to 31.0 $kgCO_2/m^2$·year, achieving a 17.1% reduction. In the colder Zone 4, also using Q23, emissions dropped from 38.8 to 32.2 $kgCO_2/m^2$·year a reduction of 17.0%. In Zone 5, Bio-PCM Q29, designed to target cooling-dominated climates, reduced emissions from 37.2 to 30.2 $kgCO_2/m^2$·year, a drop of 18.8%. Finally, Zone 6 saw the highest CO_2 intensity, where the application of Bio-PCM Q25 led to a reduction from 41.6 to 33.9 $kgCO_2/m^2$·year, equivalent to a 18.5% cut in operational emissions.

These findings are consistent with the heating and cooling demand reductions discussed in previous sections. Each Bio-PCM formulation contributed to operational CO_2 mitigation by shifting and dampening peak thermal loads, reducing compressor runtime and total electricity use.

3.4. Impact of Bio-PCM on Embodied Carbon

The embodied carbon analysis highlights significant differences between bio-based and conventional PCMs used in building envelopes. Bio-PCM M27, derived from renewable organic sources and integrated into wall and roof assemblies, exhibits an exceptionally low emission factor of 0.08 $kgCO_2/kg$, as reported in the ICE v1.6 database [24]. In contrast, commonly used synthetic and inorganic PCMs show considerably higher values: 3.75 $kgCO_2/kg$ for paraffin (C18–C28) [35], 1.53 $kgCO_2/kg$ for hydrated salt ($CaCl_2 \cdot 6H_2O$) [36], and 8.98 $kgCO_2/kg$ for stearic acid [37] as explained in Table 3. Among these, paraffin-based PCMs are the most widely used in buildings due to their favorable thermal stability, affordability, and ease of encapsulation in wallboards, gypsum plasters, and concrete composites, as demonstrated by Karaipekli et al. (2016) [38]. However, their embodied carbon remains relatively high, driven by their petroleum origin and encapsulation processes.

When comparing Bio-PCM M27 to each alternative under equal mass and integration conditions, the reduction in embodied carbon reaches approximately 97.87% compared to both stearic acid and paraffin, and 94.77% relative to hydrated salt. These results confirm the environmental superiority of Bio-PCM M27 in terms of embodied emissions. By replacing paraffin-based PCMs with bio-based formulations such as Bio-PCM M27, it is possible to reduce material-related CO_2 emissions by nearly 98% without compromising thermal storage performance, making it a highly effective strategy for advancing low-carbon building materials and meeting embodied carbon targets in sustainable construction frameworks.

Table 3. Emission factors and building applications of selected PCM types.

Type of PCM	Use in Buildings	Integrated Element	Emission Factor ($kgCO_2/kg$)	Source	Ref.
Bio-PCM M27 (Q21–Q29)	Bio-based phase change material with low embodied carbon, used in thermal storage.	Roof or Wall (boards/sheets)	0.08	ICE v1.6 database	[24]
Paraffin (C18–C28)	Stable organic PCM, often microencapsulated and integrated into plaster or concrete.	Wall or Ceiling Coatings	3.75	CarbonCloud (Paraffin wax)	[35]
$CaCl_2 \cdot 6H_2O$ (Hydrated Salt)	Inorganic PCM with high latent heat; used in wall/floor modules for heat storage.	Wall or Floor Modules	1.53	CarbonCloud ($CaCl_2$, anhydrous)	[36]
Stearic Acid (Fatty Acid)	Solid fatty acid PCM, integrated in microcapsules or sheet panels for latent storage.	Wall Inserts or Panels	8.98	CarbonCloud (Stearic acid)	[37]

4. Discussion

4.1. Alignment with Previous Studies and Contribution to the Field

Several previous investigations have addressed the integration of phase change materials (PCMs) in building envelopes to improve thermal comfort and reduce energy consumption. For instance, Salihi et al. [39] conducted a numerical study in a Moroccan semi-arid climate and demonstrated that incorporating multiple PCM layers (RT-21, RT-25, RT-28 HC) in wall assemblies can reduce annual heating and cooling loads by up to 15.2%. However, their approach focused solely on temperature fluctuation control within a limited climatic context and did not assess the embodied carbon implications or explore a nationwide zoning approach.

Similarly, Di Bari et al. [40] emphasized the environmental performance of PCMs through life cycle assessment (LCA), comparing paraffins and salt hydrates. Their multi-case LCA analysis confirmed that energy savings during the operational phase may be offset by the high embodied carbon of certain PCMs, especially petroleum-based ones like RT10HC. However, their study was mostly conducted at the material/component scale and limited to generic European climates without detailed integration into Moroccan climatic conditions.

The novelty of the present study lies in its holistic and climate-adapted approach. This research is the first to combine dynamic EnergyPlus simulations and life cycle assessment (LCA) to simultaneously assess the operational and embodied carbon impacts of bio-based PCMs in Moroccan service buildings, across six representative climate zones. Unlike prior works, this study:

- Integrates realistic hourly meteorological data for each Moroccan zone using Meteonorm, covering hot-arid, Mediterranean, Saharan, and mountainous conditions.
- Considers bio-based PCMs with low embodied carbon (e.g., 0.08 $kgCO_2/kg$), significantly outperforming conventional PCMs such as paraffin or stearic acid in both environmental and energy aspects.
- Demonstrates that specific PCM formulations (Q21–Q29) tailored to different climate profiles can reduce heating and cooling energy demands by up to 28%, and operational CO_2 emissions by up to 24%.
- Recommends zone-specific PCM types for optimal performance unlike most literature which suggests generic solutions.

Furthermore, the simulation framework was validated against the study by Hamdaoui et al. (2020) [34], showing close alignment in heating/cooling demands under similar

configurations, thereby supporting the robustness of the model. Additionally, the thermal behavior of PCMs was modeled using the enthalpy–temperature method and the CondFD solver in EnergyPlus, ensuring accurate latent heat dynamics. In summary, while prior studies either addressed thermal performance or environmental impacts in isolation, this study introduces a comprehensive, context-specific strategy that quantifies both operational and embodied carbon reductions achievable through climate-optimized bio-PCM applications in Moroccan service buildings. While experimental work remains limited in the Moroccan context, the present study contributes an innovative perspective by adapting validated bio-PCM to local climate zones. The comparative analysis with previous studies (e.g., [13,15,39,40]) confirms the robustness of the results and underlines the originality of this contribution.

Although a detailed cost–benefit analysis was not conducted in this study, it is important to note that in Morocco's centrally managed electricity system, the unit electricity price and CO_2 emission factor is uniform nationwide [20]. This implies that any reduction in operational energy demand achieved by Bio-PCM integration proportionally reduces both CO_2 emissions and electricity costs [23]. Furthermore, the embodied carbon savings observed for bio-based PCMs are intrinsically linked to lower embodied energy in the industrial production of these materials, which also suggests reduced material-related costs. Therefore, the dual benefits in terms of energy and carbon reduction indicate that bio-based PCMs present a promising and economically favorable strategy, especially when scaled in service buildings.

4.2. Recommended Bio-PCM Selection and Passive Strategy Integration

Based on dual performance indicators for heating and cooling energy demand reduction, the following Bio-PCM types are recommended for each of Morocco's six climatic zones:

- Zone 1 (Coastal–Desert): Bio-PCM Q25 is the most suitable due to its ability to balance moderate heating needs with high cooling demand.
- Zone 2 (Mediterranean): Bio-PCM Q25 remains optimal as it performs well during both the winter heating and summer cooling seasons.
- Zone 3 (Continental): Bio-PCM Q23, with its slightly lower transition temperature, better addresses the higher heating demand typical of this inland zone.
- Zone 4 (Mountainous Semi-Arid): Bio-PCM Q23 effectively targets cold conditions while still mitigating summer temperature peaks.
- Zone 5 (Hot Arid): Bio-PCM Q29 is most efficient in climates with intense summer heat, focusing on cooling performance.
- Zone 6 (Saharan): Bio-PCM Q25 offers valuable thermal regulation under the extreme diurnal temperature fluctuations characteristic of this region.

In addition, while Bio-PCM Q21 has shown excellent potential in reducing heating energy demand across all zones, its use should ideally be complemented by a passive cooling strategy to address summer loads. For example, coupling Bio-PCM Q21 with radiative sky cooling systems or green roofs as discussed in Idouanaou et al. can enhance its seasonal performance [3,41].

On the other hand, if Bio-PCM Q29 is selected primarily for its cooling benefits in hot climates (Zones 5 and 6), it is recommended to incorporate a passive heating solution to counterbalance winter demand. In such cases, Trombe walls or PV-integrated glazing systems as explored in Idouanaou et al. can effectively offset increased heating loads [4,12], contributing to a year-round energy-efficient and low-carbon building envelope.

5. Conclusions

This study confirmed that bio-based phase change materials (bio-PCMs) can significantly reduce both operational and embodied carbon emissions in Moroccan service buildings. Across all six climatic zones, notable reductions in CO_2 emissions were achieved, depending on the bio-PCM type and its thermal compatibility with each zone's conditions.

In Zone 1, Bio-PCM Q25 enabled a 24.0% reduction in operational CO_2 emissions. Zone 2 recorded a 19.5% decrease with the same PCM. In Zone 3, Bio-PCM Q23 achieved a 17.1% reduction, while Zone 4 experienced a 17.0% cut with the same formulation. In the hot-arid climate of Zone 5, Bio-PCM Q29 led to an 18.8% decrease. Finally, Zone 6 saw an 18.5% reduction using Bio-PCM Q25.

These results highlight the importance of climate-adapted PCM selection: Q25 performs best in Zones 1, 2, and 6; Q23 is optimal for Zones 3 and 4; and Q29 is most suited for Zone 5. In addition, the use of bio-sourced materials such as Bio-PCM M27, with an embodied carbon of just 0.08 $kgCO_2/kg$, provides up to 98% lower environmental impact compared to conventional PCMs. Therefore, combining climate-specific bio-PCMs with complementary passive strategies offers a promising pathway for reducing the carbon footprint of buildings in hot-climate regions like Morocco.

Future research should focus on long-term experimental validation of bio-PCM integration in Moroccan buildings, coupled with passive and active energy-saving strategies, as well as comprehensive cost–benefit analyses including transportation and end-of-life stages. From a practical perspective, the results provide a guideline for selecting climate-adapted bio-PCMs and support the development of national building codes and demonstration projects to accelerate the adoption of sustainable materials in Morocco's service building sector.

Author Contributions: Conceptualization, A.I.; Methodology, A.I.; Software, A.I.; Validation, A.I., M.M., S.K., A.B. and O.A.; Formal analysis, A.I.; Investigation, S.K., A.B., O.A., R.E.A. and O.C.; Resources, M.M.; Data curation, A.I.; Writing—original draft, A.I.; Writing—review & editing, S.K., A.B., O.A., R.E.A. and O.C.; Visualization, A.I., S.K., A.B. and O.A.; Supervision, M.M.; Project administration, M.M.; Funding acquisition, M.M. All authors have read and agreed to the published version of the manuscript.

Funding: The authors declare the following financial interests/personal relationships which may be considered as potential competing interests: This work was conducted as part of an applied research and development project within the framework of a bilateral science and technology cooperation initiative between Morocco and Hungary. The authors gratefully acknowledge the financial support provided by the Ministry of Higher Education, Scientific Research, and Innovation of the Kingdom of Morocco.

Data Availability Statement: The data that support the findings of this study are available from the corresponding author upon reasonable request.

Conflicts of Interest: The authors declare no conflicts of interest.

Abbreviations

$T_i^{j+1} - T_i^j$	Temperature at node i [K]
C_P	Specific heat capacity [J/kg·K]
ρ	Density of the material [kg/m^3]
Δ_x	Thickness of the finite difference element [m]
Δt	Time step duration [s]
k_0, k_1	Base thermal conductivity and its temperature coefficient [W/m·K]

k_i	Thermal conductivity at node iii [W/m·K]
k_w, k_E	Interfacial conductivity between nodes [W/m·K]
h_i	Enthalpy at node i [J/kg]
$HeatCap_n$	Heat capacitance of a half-node [J/m^2·K]
$Q_{Dreport,i}$	Heat flux at node i [W/m^2]
Q_{inside}	Inside face conduction heat flux [W/m^2]
$Q_{source,i}$	Internal heat source at node iii [W/m^2]
PLR	Part−load ratio (actual load/rated load)
$EIRFPLR$	EIR modifier as a function of PLR
$EIRFT$	EIR modifier as a function of temperature
$CAPFT$	Capacity modifier as a function of temperature
$\dot{Q}_{rated}$	Rated thermal capacity [W]
$\dot{Q}_{deliverd}$	Delivered thermal load [W]
COP	Coefficient of performance
$Power$	Total electric power consumption [W]
$EIR_{deforst}$	Defrost energy correction factor
$P_{crankcase}$, $P_{evap.pump}$, $P_{defrost}$	Auxiliary electric loads [W]
T_{ent}, T_{cond}	Entering and condenser air temperatures [°C]
$HREIRMod$	Heat recovery EIR modifier
$Power_{HR}$	Electric power in heat recovery mode [W]
k_{EIR}	Initial power fraction during transition
τEIR	Time constant for heat recovery transition [hr]
PCM	Phase Change Material
Bio-PCM	Bio-based Phase Change Material
LCA	Life Cycle Assessment
TES	Thermal Energy Storage
VRF	Variable Refrigerant Flow
HVAC	Heating, Ventilation, and Air Conditioning
DOAS	Dedicated Outdoor Air System
ICE	Inventory of Carbon and Energy
$HPRTF$	Heat pump runtime fraction

References

1. Li, Y.; Han, M.; Liu, S.; Chen, G. Energy consumption and greenhouse gas emissions by buildings: A multi-scale perspective. *Build. Environ.* **2019**, *151*, 240–250. [CrossRef]
2. Skillington, K.; Crawford, R.H.; Warren-Myers, G.; Davidson, K. A review of existing policy for reducing embodied energy and greenhouse gas emissions of buildings. *Energy Policy* **2022**, *168*, 112920. [CrossRef]
3. Idouanaou, A.; Malha, M.; Bah, A.; Kardellass, S. The potential of green roof strategies for reducing CO_2 emissions and energy use in Moroccan office buildings. *Green Technol. Sustain.* **2025**, *3*, 100177. [CrossRef]
4. Idouanaou, A.; Malha, M.; Bah, A.; Ansari, O. The Role of PV-Integrated Double-Skin Facades in Achieving Net-Zero Carbon Emissions in Commercial Buildings in Morocco. *EPJ Web Conf.* **2025**, *326*, 02003. [CrossRef]
5. Baylis, C.; Cruickshank, C.A. Review of bio-based phase change materials as passive thermal storage in buildings. *Renew. Sustain. Energy Rev.* **2023**, *186*, 113690. [CrossRef]
6. Liu, L.; Fan, X.; Zhang, Y.; Zhang, S.; Wang, W.; Jin, X.; Tang, B. Novel bio-based phase change materials with high enthalpy for thermal energy storage. *Appl. Energy* **2020**, *268*, 114979. [CrossRef]
7. Benhorma, A.; Bensenouci, A.; Teggar, M.; Ismail, K.; Arıcı, M.; Mezaache, E.; Laouer, A.; Lino, F. Prospects and challenges of bio-based phase change materials: An up to date review. *J. Energy Storage* **2024**, *90*, 111713. [CrossRef]
8. Bruno, R.; Bevilacqua, P. Bio-PCM to enhance dynamic thermal properties of dry-assembled wooden walls: Experimental results. *Build. Environ.* **2023**, *242*, 110526. [CrossRef]
9. Zhan, H.; Mahyuddin, N.; Sulaiman, R.; Khayatian, F. Phase change material (PCM) integrations into buildings in hot climates with simulation access for energy performance and thermal comfort: A review. *Constr. Build. Mater.* **2023**, *397*, 132312. [CrossRef]
10. Fabiani, C.; Pisello, A.L.; Barbanera, M.; Cabeza, L.F. Palm oil-based bio-PCM for energy efficient building applications: Multipurpose thermal investigation and life cycle assessment. *J. Energy Storage* **2020**, *28*, 101129. [CrossRef]

11. Idouanaou, A.; Malha, M.; Bah, A.; Kardellass, S. Influence of Leaf Area Index and Plant Height on Green Roof Carbon Footprint in Moroccan Residential Buildings in Hot Climates. *EPJ Web Conf.* **2025**, *326*, 05004. [CrossRef]
12. Idouanaou, A.; Cherqi, O.; Malha, M.; Bah, A. Impact of Shading and Glazing Types of Trombe Walls on the Carbon Footprint of Residential Buildings in Morocco. *E3S Web Conf.* **2024**, *572*, 03002. [CrossRef]
13. Kosny, J.; Kossecka, E.; Brzezinski, A.; Tleoubaev, A.; Yarbrough, D. Dynamic thermal performance analysis of fiber insulations containing bio-based phase change materials (PCMs). *Energy Build.* **2012**, *52*, 122–131. [CrossRef]
14. Anter, A.G.; Sultan, A.A.; Hegazi, A.; El Bouz, M. Thermal performance and energy saving using phase change materials (PCM) integrated in building walls. *J. Energy Storage* **2023**, *67*, 107568. [CrossRef]
15. Guermat, Z.; Kabar, Y.; Kuznik, F.; Boukelia, T. Numerical investigation of the integration of new bio-based PCM in building envelopes during the summer in Algerian cities. *J. Energy Storage* **2024**, *79*, 110111. [CrossRef]
16. Jin, X.; Medina, M.A.; Zhang, X. On the importance of the location of PCMs in building walls for enhanced thermal performance. *Appl. Energy* **2013**, *106*, 72–78. [CrossRef]
17. Öztürk, G.; Temiz, A.; Hekimoğlu, G.; Aslan, M.; Demirel, G.K.; Erdeyer, Ö.N.; Sarı, A.; Gencel, O.; Subaşı, S. Microencapsulated phase change material/wood fiber-starch composite as novel bio-based energy storage material for buildings. *J. Energy Storage* **2024**, *84*, 110911. [CrossRef]
18. Boussaba, L.; Foufa, A.; Makhlouf, S.; Lefebvre, G.; Royon, L. Elaboration and properties of a composite bio-based PCM for an application in building envelopes. *Constr. Build. Mater.* **2018**, *185*, 156–165. [CrossRef]
19. Jin, X.; Zhang, S.; Xu, X.; Zhang, X. Effects of PCM state on its phase change performance and the thermal performance of building walls. *Build. Environ.* **2014**, *81*, 334–339. [CrossRef]
20. Programme for Energy Efficiency in Buildings. Efficacité Énergétique dans les Bâtiments au Maroc–Support de Sensibilisation. 2022. Available online: https://peeb.build/wp-content/uploads/2024/12/PEEB__efficacite-energetique-dans-les-batiments-au-maroc__support-de-sensibilation_.pdf.pdf (accessed on 15 April 2025).
21. Meteonorm Software. Données Climatiques par Meteonorm. Available online: https://meteonorm.com/ (accessed on 13 July 2023).
22. *ISO 6946:2007*; Building Components and Building Elements. Organisation Internationale de Normalisation: Geneva, Switzerland, 2020.
23. The Mohammed VI Foundation for Environmental Protection. Bilan Carbone Maroc. Available online: https://www.bilancarbonemaroc.org/ (accessed on 7 April 2025).
24. Hammond, G. *Inventory of Carbon & Energy (ICE)*; University of Bath: Bath, UK, 2006.
25. EnergyPlus. Adaptive Convection Algorithm. Available online: https://bigladdersoftware.com/epx/docs/8-1/engineering-reference/page-021.html#adaptive-convection-algorithm (accessed on 26 February 2024).
26. Idouanaou, A.; Malha, M.; Bah, A. Evaluating the influence of convective heat transfer coefficient on the carbon footprint of a service building in Morocco. *E3S Web Conf.* **2024**, *579*, 02005. [CrossRef]
27. Beausoleil-Morrison, I. The adaptive simulation of convective heat transfer at internal building surfaces. *Build. Environ.* **2002**, *37*, 791–806. [CrossRef]
28. Beausoleil-Morrison, I. The Adaptive Coupling of Heat and Air Flow Modeling within Dynamic Whole-Building Simulations. Ph.D. Thesis, University of Strathclyde, Glasgow, UK, 2000. Available online: https://stax.strath.ac.uk/concern/theses/4q77fr43v (accessed on 20 April 2024).
29. Pedersen, C. Enthalpy formulation of conduction heat transfer problems involving latent heat. *Simulation* **1972**, *18*, 57–59. [CrossRef]
30. Tabares-Velasco, P.C.; Christensen, C.; Bianchi, M.; Booten, C. Verification and Validation of EnergyPlus Conduction Finite Difference and Phase Change Material Models for Opaque Wall Assemblies. 2012. Available online: http://www.osti.gov/bridge (accessed on 15 April 2025).
31. Hong, T.; Sun, K.; Zhang, R.; Hinokuma, R.; Kasahara, S.; Yura, Y. Development and validation of a new variable refrigerant flow system model in EnergyPlus. *Energy Build.* **2016**, *117*, 399–411. [CrossRef]
32. Raustad, R. A Variable Refrigerant Flow Heat Pump Computer Model in EnergyPlus. ASHRAE Transactions, 2013. Available online: https://publications.energyresearch.ucf.edu/wp-content/uploads/2018/06/FSEC-CR-1950-13.pdf (accessed on 23 April 2024).
33. EnergyPlus. Environmental Impacts. Available online: https://bigladdersoftware.com/epx/docs/8-0/engineering-reference/page-121.html#environmental-impacts (accessed on 30 December 2024).
34. Hamdaoui, S.; Mahdaoui, M.; Allouhi, A.; El Alaiji, R.; Kousksou, T.; El Bouardi, A. Energy demand and environmental impact of various construction scenarios of an office building in Morocco. *J. Clean. Prod.* **2018**, *188*, 113–124. [CrossRef]
35. CarbonCloud. Paraffin wax 3.75 kg CO_2e/kg. 2025. Available online: https://apps.carboncloud.com/climatehub/product-reports/id/453411129460 (accessed on 15 April 2025).

36. CarbonCloud. Calcium chloride (CaCl2). E509 1.53 kg CO_2e/kg. 2025. Available online: https://apps.carboncloud.com/climatehub/product-reports/id/146255465878 (accessed on 15 April 2025).
37. CarbonCloud. Stearic acid. E570 8.98 kg CO_2e/kg. 2025. Available online: https://apps.carboncloud.com/climatehub/product-reports/id/3611333312577 (accessed on 15 April 2025).
38. Karaipekli, A.; Sarı, A.; Biçer, A. Thermal regulating performance of gypsum/(C18–C24) composite phase change material (CPCM) for building energy storage applications. *Appl. Therm. Eng.* **2016**, *107*, 55–62. [CrossRef]
39. Salihi, M.; El Fiti, M.; Harmen, Y.; Chhiti, Y.; Chebak, A.; Alaoui, F.E.M.; Achak, M.; Bentiss, F.; Jama, C. Evaluation of global energy performance of building walls integrating PCM: Numerical study in semi-arid climate in Morocco. *Case Stud. Constr. Mater.* **2022**, *16*, e00979. [CrossRef]
40. Di Bari, R.; Horn, R.; Nienborg, B.; Klinker, F.; Kieseritzky, E.; Pawelz, F. The environmental potential of phase change materials in building applications. A multiple case investigation based on life cycle assessment and building simulation. *Energies* **2020**, *13*, 3045. [CrossRef]
41. Cherqi, O.; Idouanaou, A.; Malha, M.; Kardellass, S. Numerical modeling and experimental study of SiO2 radiative cooling coatings on aluminum substrate in humid conditions: A case study in Morocco Mediterranean climate. *Energy Build.* **2025**, *339*, 115771. [CrossRef]

Disclaimer/Publisher's Note: The statements, opinions and data contained in all publications are solely those of the individual author(s) and contributor(s) and not of MDPI and/or the editor(s). MDPI and/or the editor(s) disclaim responsibility for any injury to people or property resulting from any ideas, methods, instructions or products referred to in the content.